Paleoseismicity derived from piston-coring methods, Explorer and Juan de Fuca plate systems, British Columbia

M. Riedel and K.W. Conway

2015

Paleoseismicity derived from piston-coring methods, Explorer and Juan de Fuca plate systems, British Columbia

M. Riedel and K.W. Conway

2015

A copy of this publication is also available for reference in depository
libraries across Canada through access to the Depository Services Program's
Web site at http://dsp-psd.pwgsc.gc.ca

This publication is available for free download through GEOSCAN
http://geoscan.nrcan.gc.ca

Authors
M. Riedel (mriedel@geomar.de)
K.W. Conway (Kim.Conway@canada.ca)
Geological Survey of Canada
9860 West Saanich Road
Vancouver, British Columbia
V8L 4B2

M. Riedel (mriedel@geomar.de)
Present address:
GEOMAR Helmholtz
Centre for Ocean Research
Kiel, Wischhofstrasse 1-3, 24148 Kiel, Germany

Correction date:

Paleoseismicity derived from piston-coring methods, Explorer and Juan de Fuca plate systems, British Columbia

Abstract: Coring of marine sediments has revealed deposits related to slope instability induced by seismicity on the western margin of Canada. Debris flows and turbidite sequences related to megathrust earthquakes have been recovered in six piston cores on the Juan de Fuca and Explorer tectonic plates, allowing comparison of the response of each plate to shaking during great earthquakes. Analyses of the recovered cores show that turbidite sequences associated with a megathrust quake occur on the Juan de Fuca Plate and do not occur in cores collected 90 km away at a similar site on the Explorer Plate. The record of subduction-related earthquake turbidite sequences is not complete at the Juan de Fuca study area and no reconstruction of megathrust quake periodicity is thus possible using this site alone. These results indicate that strong ground shaking is probably not experienced during large subduction earthquakes on the Explorer Plate.

Résumé : Le carottage de sédiments marins a révélé la présence de dépôts rattachés à l'instabilité de talus engendrée par l'activité sismique le long de la marge continentale de l'Ouest du Canada. Des coulées de débris et des séquences turbiditiques rattachées à des mégaséismes de chevauchement ont été reconnues dans les carottes de six échantillons prélevés par un carottier à piston à la surface des plaques tectoniques Juan de Fuca et Explorer, permettant ainsi de comparer la réponse aux secousses de chaque plaque lors de forts tremblements de terre. Des analyses des carottes prélevées ont révélé que des séquences turbiditiques associées à un mégaséisme de chevauchement sont présentes sur la plaque Juan de Fuca, mais absentes des carottes prélevées 90 km plus loin en un site semblable sur la plaque Explorer. Le registre des séquences turbiditiques engendrées par des séismes de subduction est incomplet dans la zone d'étude de la plaque Juan de Fuca, de sorte qu'il n'est pas possible de réaliser une reconstitution permettant de définir la périodicité des mégaséismes de chevauchement en se basant uniquement sur l'examen de ce site. Nos résultats montrent que de fortes secousses ne se manifestent probablement pas à la surface de la plaque Explorer lors de forts séismes de subduction.

INTRODUCTION

As part of the Public Safely Geoscience Program in natural hazards research the Geological Survey of Canada undertakes studies in support of the effective management of natural hazards such as earthquake seismicity, slope instability, tsunamis, and near-surface fault rupture. In order to assess the ongoing regional risk of earthquakes along the west coast of Canada, knowledge of the past history and periodicity of large earthquakes is critical. The relationship between turbidite occurrence and the periodicity of megathrust earthquakes has been established by studies undertaken along the south-central Cascadia subduction zone in the past several decades (Adams, 1990; Goldfinger et al., 2003, 2012). Similar studies of the northern portion of the subduction zone have recently begun (Hamilton et al., 2015) and details of how subduction zone rupture occurs during each large seismic event along the entire length of the active margin are under investigation.

As part of the Seafloor Earthquake Array–Japan-Canada Cascadia Experiment (SeaJade-II) conducted in December 2013, coring was undertaken at submarine landslides to study the recurrence of megathrust earthquakes on the Cascadia subduction zone and on the Explorer Plate, north of the Nootka fault zone (Riedel et al., 2014). An overview of the setting of the margin and the location of the two submarine landslides is shown in Figure 1, together with the location of the 35 ocean bottom seismometers deployed.

The work conducted during the SeaJade-II mission is a continuation of work started in 2008 during the expedition 2008007PGC (R. Haacke, T. Hamilton, R. Enkin, L. Esteban, and J. Pohlman, unpub. report, 2008) and recently summarized in Hamilton et al. (2015). While deploying the grid of ocean bottom seismometers and following the cruise track between ocean bottom seismometer stations, the vessel covered regions of known submarine landslides, which have been identified from high-resolution bathymetric maps (K. Naegeli, unpub. report, 2010). They have not yet been studied in detail for understanding of submarine slope-failure processes, as well as their potential to record a history of failure deposits related to large earthquake shaking. Two general types of submarine slope failures can be identified on the margin: blocky slides and debris-flow–type slides (Fig. 1). Blocky slides (e.g. Slipstream) show intact slide material, whereas the debris-flow–type (e.g. Orca) slides show incoherent outrunner failure masses. Two of the eight landslides identified by K. Naegeli (unpub. report, 2010) were investigated in 2008 in detail during expedition 2008007PGC (R. Haacke, T. Hamilton, R. Enkin, L. Esteban, and J. Pohlman, unpub. report, 2008) and two transects of cores were recovered across the failure mass of Orca and Slipstream (Hamilton et al., 2015). The deforming late Pleistocene sediments that are the source of the failures are more than 250 m thick in this area (Riedel et al., 2006;
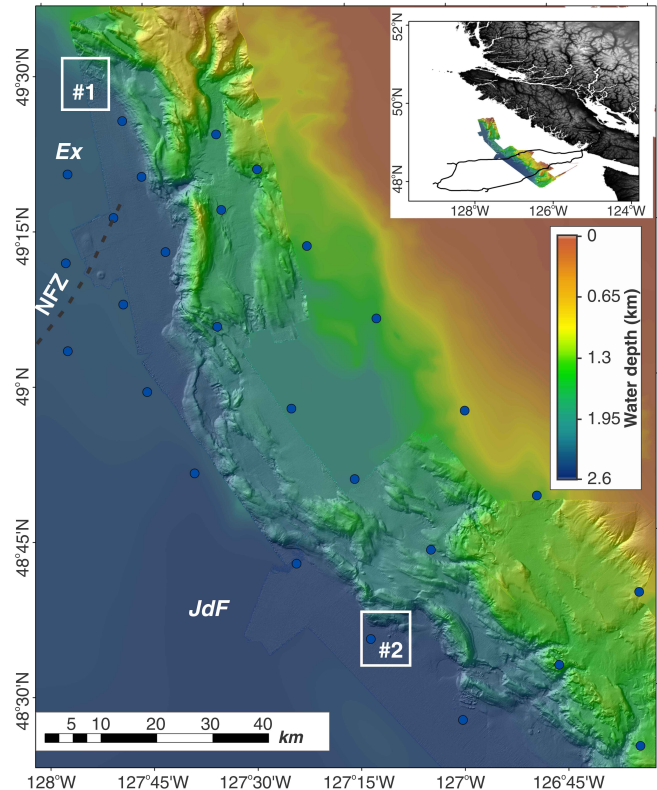
Figure 1. Map showing bathymetry and shaded relief of the north Cascadia margin offshore Vancouver Island (data courtesy D. Kelly, University of Washington). Ocean-bottom seismometer locations of the SeaJade-II mission are shown as blue circles. The two locations of piston coring are outlined with small white rectangles. A detailed map of each region is shown in Figures 2 and 3. Ex = Explorer Plate, JdF = Juan de Fuca Plate, NFZ = Nootka fault zone

Hamilton et al., 2015) and form the frontal ridge and underlie the seabed on the lower continental slope (Hamilton et al., 2015).

METHODS

Marine geoscience surveys were undertaken during the SeaJade-II Expedition on board Canadian Coast Guard Ship (CCGS) *John P. Tully* cruise 2013007PGC in November 2013. Prior to the expedition, a subset of submarine landslides was identified as possible targets as they are close to an ocean-bottom seismometer location and 3.5 kHz subbottom profiler data were acquired across these features during the ocean-bottom seismometer deployment. The data were then interpreted together with bathymetry onboard, and slide locations were ranked according to their potential for yielding cores with a turbidite record for reconstructing a history of large earthquake shaking. Two slides were chosen for taking additional piston cores. The first slide targeted for coring is located north of the Nootka fault zone on the Explorer

Plate and the second slide complex is located north of Orca and Slipstream slides on the Juan de Fuca Plate, at a site designated Otter slide. Cores were collected using a Benthos split-piston coring system with a 1000 kg head weight and barrel assemblies up to 12 m (Fig. 2). Two multisensor core logger systems were used to analyze the cores for physical properties including gamma-ray density, magnetic suscepti-bility, and high-resolution image data collection. Cores were split and visually described. Foraminifera from fractions of sieved subsamples were obtained and accelerator mass-spectroscopy radiocarbon dating was undertaken at Beta Analytic Inc. (Miami, Florida). Ages are presented and discussed in conventional radiocarbon years BP (BP). A reservoir correction of 800 a was applied. Radiocarbon age calibration was accomplished with the program OxCal version 4.1.7 (Bronk Ramsey, 2009).

The hull-mounted 3.5 kHz subbottom profiler was used to image across most of the known submarine slide failures occurring in between the grid of 35 ocean-bottom seismometers. The system provides an image of subsea-floor acoustic reflectivity with a vertical resolution of about 0.2–0.5 m (depending on sediment velocity); however, as a hull-mounted system, the sounder is prone to any ship movement (pitch and roll) that degrades the image, especially at higher vessel speed. The data were acquired whenever possible at a speed of about 4 knots (~8 km/h).

RESULTS

At each location three piston cores were recovered along a transect upslope, covering the distal portion of the outrun-ner material to the zone close to the head scarp. The trigger core for each piston core was also recovered and archived, but no samples were taken for analysis. Core locations are show in Table 1 and core recovery is summarized in Table 2. Radiocarbon ages for all subsamples taken are listed in Table 3. Coring was attempted in water depths of 2100–2400 m for the slide on the Explorer Plate, and 2300–2500 m for Otter slide on the Juan de Fuca Plate. Core deployment (and recovery) in these water depths is between 35 minutes and 45 minutes (winch speed of ~1 m/s). Location of the core on the seafloor is therefore known only to within 50 m. The ship's position at the time of core deployment on deck and when the piston core hit bottom (Table 1) was recorded. Core location is assigned to the average of both locations assuming that the coring wire did not drift much laterally away from the vessel due to ocean currents.
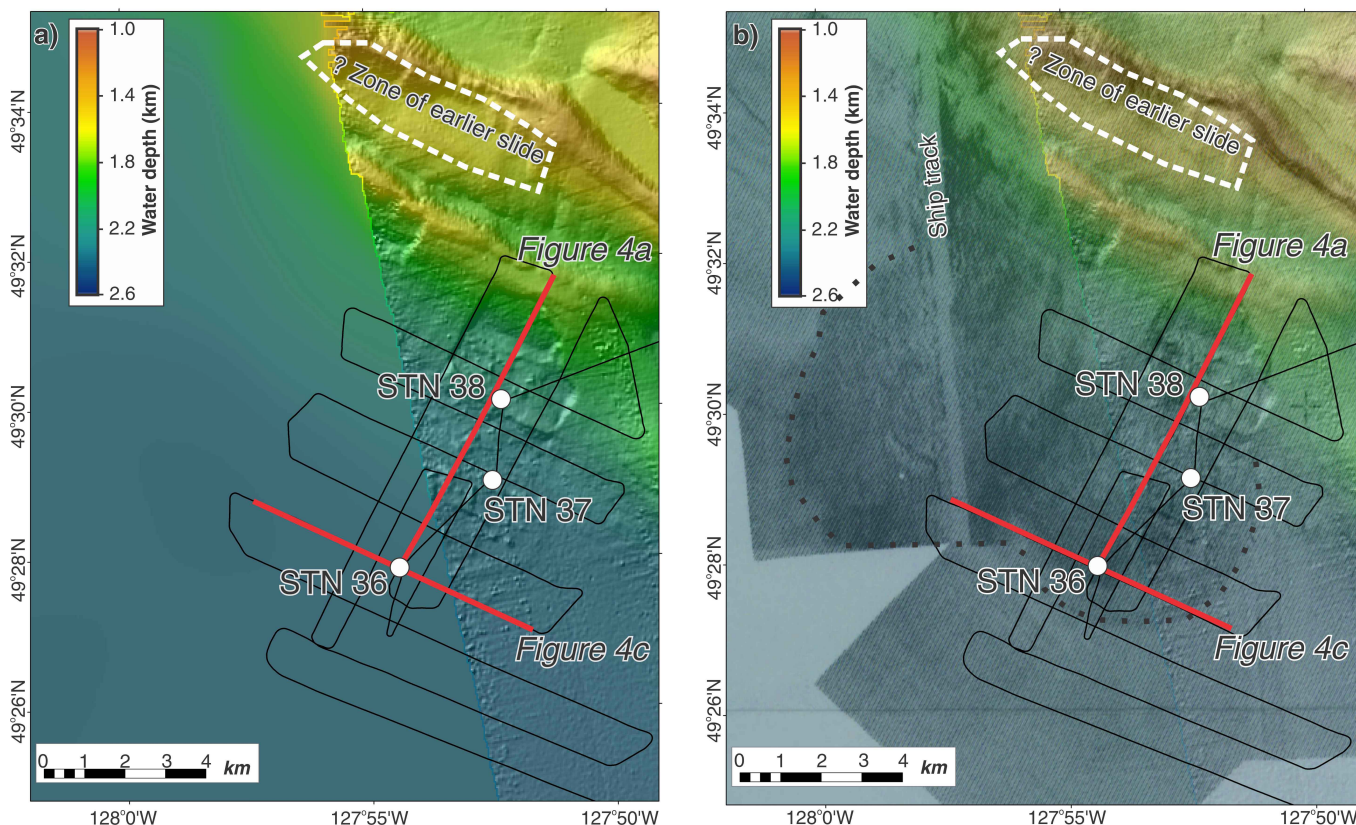
Figure 2. a) Location of coring area 1 on the Explorer Plate showing water depth, shaded multibeam relief, sites of piston coring (stations 36–38), as well as profiles acquired with the 3.5 kHz subbottom profiler. **b)** Location of coring area 1 on the Explorer Plate showing backscatter (high backscatter is black) across the double-slide complex (*modified from* Davis et al., 1987a), sites of piston coring (stations 36–38), as well as profiles acquired with the 3.5 kHz subbottom profiler. Water depth is also shown (with 70% transparency). STN = station

Table 1. Location and details of operation of piston cores. STN = station

Date and time (UTC)	Latitude	Longitude	Event
2013/12/04 17:56:29	49.465025	127.906083	Core 1 deployed
2013/12/04 18:38:28	49.465335	127.906125	Core 1 at bottom
	49.46518	127.906104	*Average location* Core 1, STN 36
2013/12/04 21:08 :45	49.483457	127.875253	Core 2 deployed
2013/12/04 21:54:44	49.483711	127.875569	Core 2 at bottom
	49.483584	127.875411	*Average location* Core 2, STN 37
2013/12/04 23:49:16	49.502477	127.871170	Core 3 deployed
2013/12/05 00:28:08	49.502515	127.871169	Core 3 at bottom
	49.502496	127.8711695	*Average location* Core 3, STN 38
2013/12/05 17:00:10	48.580474	127.168352	Core 4 deployed
2013/12/05 17:41:25	48.580834	127.168872	Core 4 at bottom
	48.580654	127.168536	*Average location* Core 4, STN 39
2013/12/05 19:26:15	48.589210	127.167579	Core 5 deployed
2013/12/05 20:08:16	48.589177	127.167854	Core 5 at bottom
	48.5891935	127.1677165	*Average location* Core 5, STN 40
2013/12/05 22:33:38	48.603839	127.164948	Core 6 deployed
2013/12/05 23:33:47	48.603674	127.165659	Core 6 at bottom
	48.6037565	127.1653035	*Average location* Core 6, STN 41

Table 2. Core recovery information for piston cores and trigger (gravity) cores.

Core	Section	Label	Length (cm)	Extra pieces
Piston core #1	1	A-B	152	Cone-nose, cutting-shoe, core catcher
	2	B-C	152	
	3	C-D	152	
	4	D-E	152	
	5	E-F	101	
	Total		709	
Trigger core #1	1	A-B	89	No samples in cutter or catcher
Piston core #2	1	A-B	152	No samples in cutter or catcher
	2	B-C	152	
	3	C-D	152	
	4	D-E	51	
	Total		507	
Trigger core #2	1	A-B	134	No samples in cutter or catcher
Piston core #3	1	A-B	152	Core cutter + catcher
	2	B-C	152	
	3	C-D	17	
	Total		321	
Trigger core #3	1	A-B	78	No samples in cutter or catcher
Piston core #4	1	A-B	152	
	2	B-C	152	
	3	C-D	152	
	4	D-E	110	
	Total		566	
Trigger core #4	1	A-B	88	No samples in cutter or catcher
Piston core #5	1	A-B	152	
	2	B-C	67	
	Total		219	
Trigger core #5	1	A-B	10	No samples in cutter or catcher
Piston core #6	1	A-B	152	
	2	B-C	69	
	Total		221	
Trigger core #6	1	A-B	76	No samples in cutter or catcher

Multibeam and backscatter data at core locations

Explorer Plate slide

The first area targeted for piston coring was the site of a double failure complex, only partially imaged with modern multibeam data (*see* Fig. 2a). The slide appears similar in size and shape to Slipstream slide (R. Haacke, T. Hamilton, R. Enkin, L. Esteban, and J. Pohlman, unpub. report, 2008; K. Naegeli, unpub. report, 2010; Hamilton et al., 2015) with sharp, rectangular edges and a debris field with several large blocks downslope. North of the sharp-looking edges of the recent head scar an older, eroded surface can be seen, likely associated with an earlier slide event (outlined by a dashed white line in Fig. 2a, b). The backscatter data from Davis et al. (1987a) showed two aprons of high-backscatter regions (Fig. 2b). The event located to the east is linked to the zone of sharp edges and runs out to a distance of about 1 km beyond coring station 36, whereas the event located to the

west appears to have originated from a more elongate source region. The northward-located zone of a speculated older slide surface shows no high backscatter.

Juan de Fuca Plate slide

The area chosen for piston coring is about 18 km to the northwest of previous coring efforts around Slipstream slide (Hamilton et al., 2015). Multibeam data show a semicircular slide scar on the frontal ridge (Fig. 3a) with some outrunner material up to 2.5 km downslope of the head scarp at the frontal ridge (measured up to a large intact block). The

UCIAMS	Sample name	^{14}C age (BP)	±	From	To	Cal ^{14}C (BP)	±
154164	STN 0036 270 cm	19590	70	22896	22436	22652	121
154165	STN 0036 450 cm	15690	60	18321	17891	18102	111
154166	STN 0036 460 cm	19560	160	23040	22315	22653	187
154167	STN 0036 640 cm	8755	35	9108	8705	8915	100
154168	STN 0036 680 cm	23230	120	27141	26327	26736	210
154169	STN 0037 370 cm	22300	100	26006	25587	25798	105
154170	STN 0037 490 cm	9400	80	10015	9472	9714	140
154171	STN 0038 125 cm	28160	360	32114	30776	31344	327
154172	STN 0039 38 cm	1930	15	1216	957	1085	66
154173	STN 0039 53 cm	2155	20	1415	1181	1308	54
154174	STN 0039 85 cm	4280	20	4004	3678	3846	81
154175	STN 0039 110 cm	8020	25	8194	7949	8077	64
154176	STN 0039 375 cm	10075	40	10742	10387	10568	87
154717	STN 0036 240 cm	5125	50	5217	4816	4988	108
154718	STN 0038 90 cm	2790	100	2308	1770	2032	139

backscatter data (Davis et al., 1987b) show an apron of high backscatter up to 3.5 km from the head scarp, indicating that some finer material was deposited further downslope onto the abyssal plain (Fig. 3b). Core station 39 is within, but at the outer limit of the apron of outrunner material defined from the backscatter image.
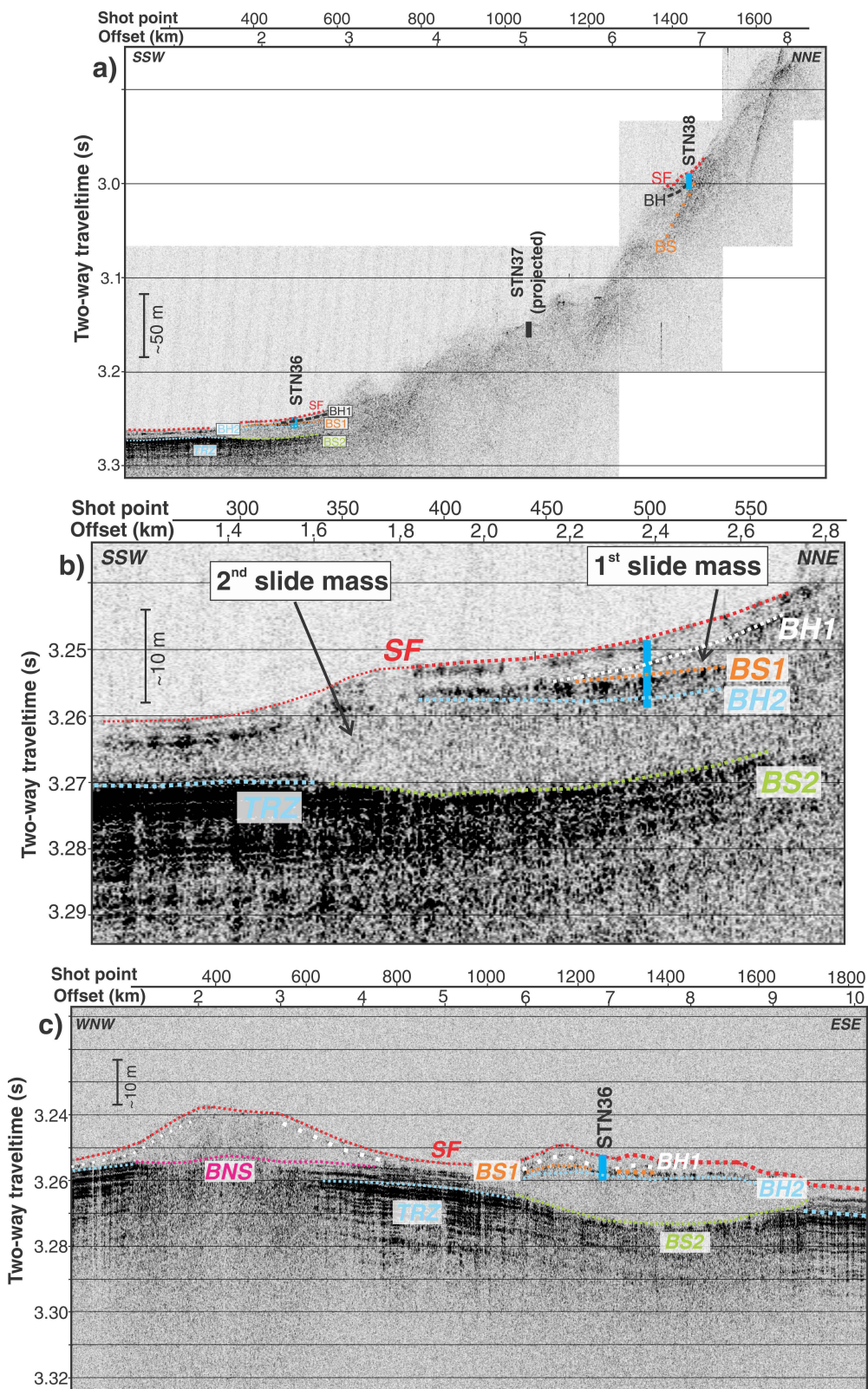
Subbottom profiler data and core sites

Explorer Plate, core stations 36–38

A total of 12 lines of 3.5 kHz data were acquired across the slide complex on the Explorer Plate (Fig. 2a, b). Three locations were chosen onboard based on those data and the multibeam image available. A transect of three cores along a central line of 3.5 kHz data are shown in Figure 4a. The steep topography makes imaging difficult; however, at core stations 36 and 38, penetration and resolution of the data are sufficient to identify major layers and slide masses that are also seen in the core data. At core station 36 toward the frontal lobe of the slide mass, two slumps were intersected by the piston core. The uppermost slump mass is relatively thin and underlain by about 2 m of Holocene material. Only
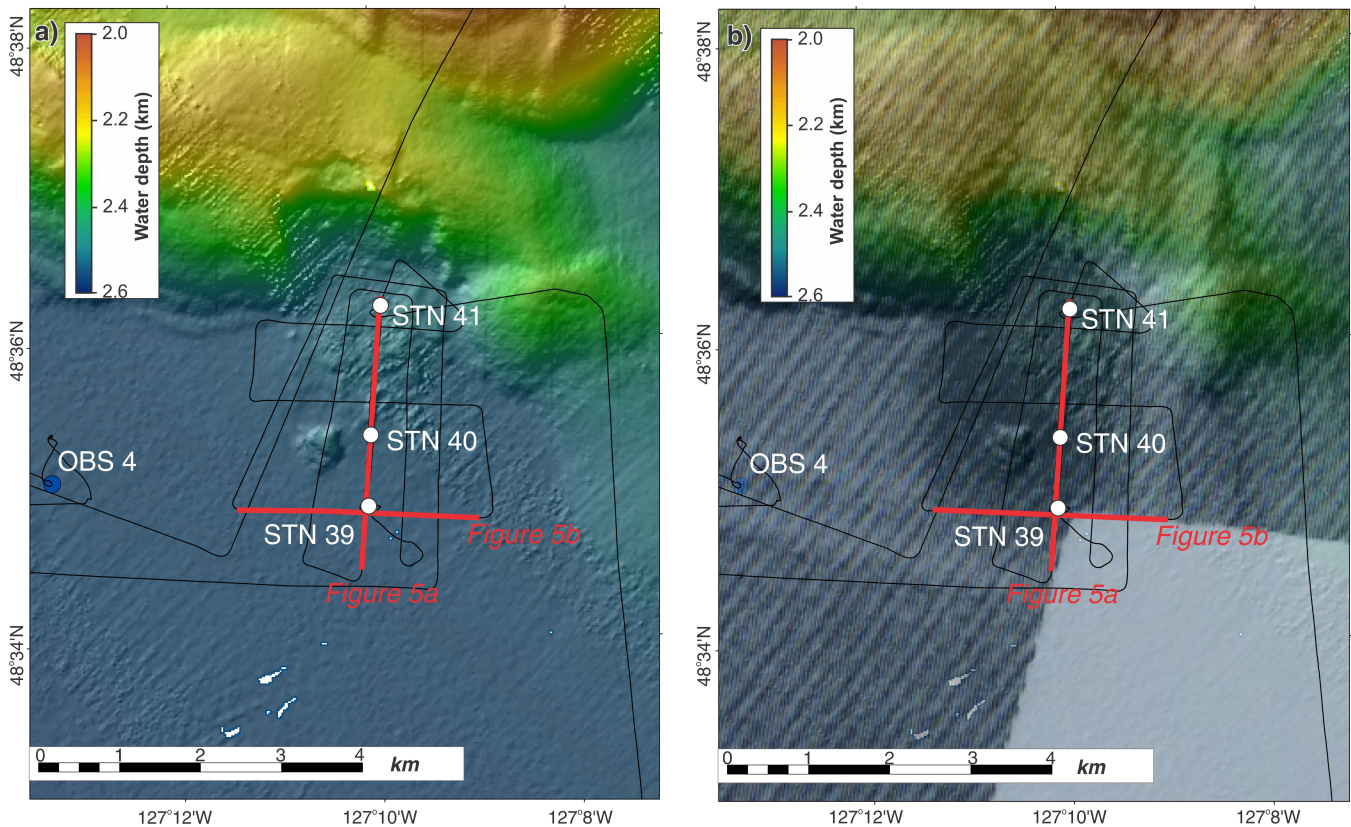
Figure 3. a) Location of coring area 2 on the Juan de Plate showing water depth, shaded multibeam relief, sites of piston coring (stations 39–41), as well as profiles acquired with the 3.5 kHz subbottom profiler. **b)** Location of coring area 2 on the Juan de Fuca Plate showing backscatter (high backscatter is black) across the complex (*modified from* Davis et al., 1987b), sites of piston coring (stations 39–41), as well as profiles acquired with the 3.5 kHz subbottom profiler. Water depth is also shown (with 70% transparency). STN = station, OBS = ocean-bottom seismometer

Figure 4. a) Subbottom profiler data acquired downslope of the slide scar at coring area 1 on the Explorer Plate with core position station 36 superimposed. Two slide masses can be imaged, with some layered sediments in between. Compare to Figure 4b for details on core station 36. **b)** Subbottom profiler data acquired downslope of the slide scar at coring area 1 on the Explorer Plate with core position station 36 superimposed. Two slide masses can be imaged, with some layered sediments in between (compare to core descriptions in section 3). **c)** Subbottom profiler data through core station 36 on the Explorer Plate with coring position superimposed showing the double-slide complex. SF = seafloor (red), BH1 = Base of Holocene 1 (white), BH2 = Base of Holocene 2 (blue), BS1 = base of slumps 1 (orange), BS2 = base of slump 2 (green), TRZ = top of reflective zone (light blue), BNS = base of northwestern slump (magenta), STN = station

the top few centimetres of the lower slide mass were recovered in core station 36. Farther upslope at core station 38, the 3.5 kHz data show one slide mass underneath a cover of Holocene sediment. The base of the slump dips steeply downslope, whereas the Holocene material forms a uniform drape on top of the mass. In the perpendicular direction through core station 36 (Fig. 4c), are visible the northwestern (not cored) and the southeastern slide mass. Both masses do not seem to overlap at this distance away from the respective slide scars. A uniform drape of Holocene sediments (~2 m thick) can be mapped across both slide masses; however, at the second, northwestern slide mass the intermittent layer of Holocene sediments appears absent.

Juan de Fuca Plate, core stations 39–41

At Otter slide, a total of nine lines of 3.5 kHz data were acquired (Fig. 3a, b) to image the slide mass. A central line through the core transect is shown in Figure 5a. At the distal part of the slide mass (core station 39) a small wedge of a slump material can be identified, covered by a drape of Holocene sediments. The wedge of slump material is underlain again by stratified sediments (Fig. 5b). At core station 40, only a drape of layered sediment on top of a massive slide mass can be identified. Due to the steep topography near core station 41 and related side echoes, imaging around core station 41 is heavily compromised. At this location, as well as at the Explorer Plate coring area 1, a highly reflective zone of layered sediment is found. This layer, approximately at 4–6 m below the seafloor, may be the base of the Holocene (top of Pleistocene).

Core description and physical property data

Juan de Fuca Plate, core stations 39–41

Core lithology recovered at core stations 39, 40, and 41 showed that two debris-flow intervals were penetrated by the cores (Fig. 6). The massive and mixed and deformed debris-flow sequences are easily distinguished from hemipelagic accumulations. Graded fine sand beds interrupt the hemipelagic sediments at six levels in core station 39. These graded beds have sharp bases and are higher in magnetic susceptibility and have higher gamma-ray density than the enclosing sediments. The sand beds are numbered for ease of identification in Figure 6. Station 40 did not recover turbidite sequences, whereas station 41 possibly contained one turbidite. Only thin recent (Holocene) sections were recovered in cores 40 and 41. The subbottom profiles of the cored sections are imaged in Figure 5a and 5b. Core 39 can be seen to penetrate the distal part of the massive slide unit, whereas cores 40 and 41 sit directly on the thick (>40 m) slide mass.

Explorer Plate, core stations 36–38

As many as four units were recovered in cores from the Explorer Plate site (Fig. 7). A basal unit composed of deformed clay beds and distorted layers is seen in core station 36 and 39 from the Juan de Fuca Plate slide. The core images show the unit to be a mixture of grey and olive muds that have been mixed. Radiocarbon ages indicate that the distorted unit is dated at between 28 160 BP and 18 102 BP. This unit is overlain in all cases by a bioturbated massive mud that is dated to between 8915 BP and 2790 BP. Cores recovered at the Explorer Plate sites contained one or two debris-flow–type slides separated or capped by recent hemipelagic sediments (Fig. 6). Gamma-ray density is much higher in the debris-flow units than in the hemipelagic mud units.

DISCUSSION

The Otter slide is a clear and significant failure on the multibeam and in subbottom profile data. The geological units sampled in the cores are clearly of very different lithologies. At the Otter slide site on the Juan de Fuca Plate, turbidite-hosting laminated intervals bracket an intermixed and remolded grey and green unit. The remolded unit is imaged as the massive unit defined in subbottom profile data in Figures 5a and 5b. The unit is a mixture of glacial sediments and olive clay units that appear similar to recent sediments in colour and texture. This suggests that the slide originated in glacial clay-rich sediments and incorporated recent sediments as the debris flow moved downslope. The turbidite sequences as well as the debris flows would probably have been events triggered during earthquakes as is the case at other sites along the Cascadia deformation front (Hamilton et al., 2015). The Otter slide is isolated from uphill sources of turbidite materials by the ridges and local morphology of the deforming front. The coring sites are therefore protected from direct connection to the slope so delivery of sediment to the site is restricted to local events only (Fig. 2).

The uppermost turbidite occurs after 1308 ± 54 BP and before 1086 ± 66 BP. In the Slipstream slide cores (Hamilton et al., 2015) the turbidite record is complete until the mid-Holocene. The megathrust earthquake recurrence interval calculated from the Slipstream slide study was 394 ± 126 a. As only three events are recorded by the Otter Slide cores after 8077 ± 64 BP it is clear that many events are missing from the local record and that no similar reconstruction for even a portion of the Holocene would be possible using this site alone.

The slides of glacial sediments are probably related to seismic events as is the case for nearby slides such as Slipstream slide (Hamilton et al., 2015). Many slides are located along the margin of the deformation front that has
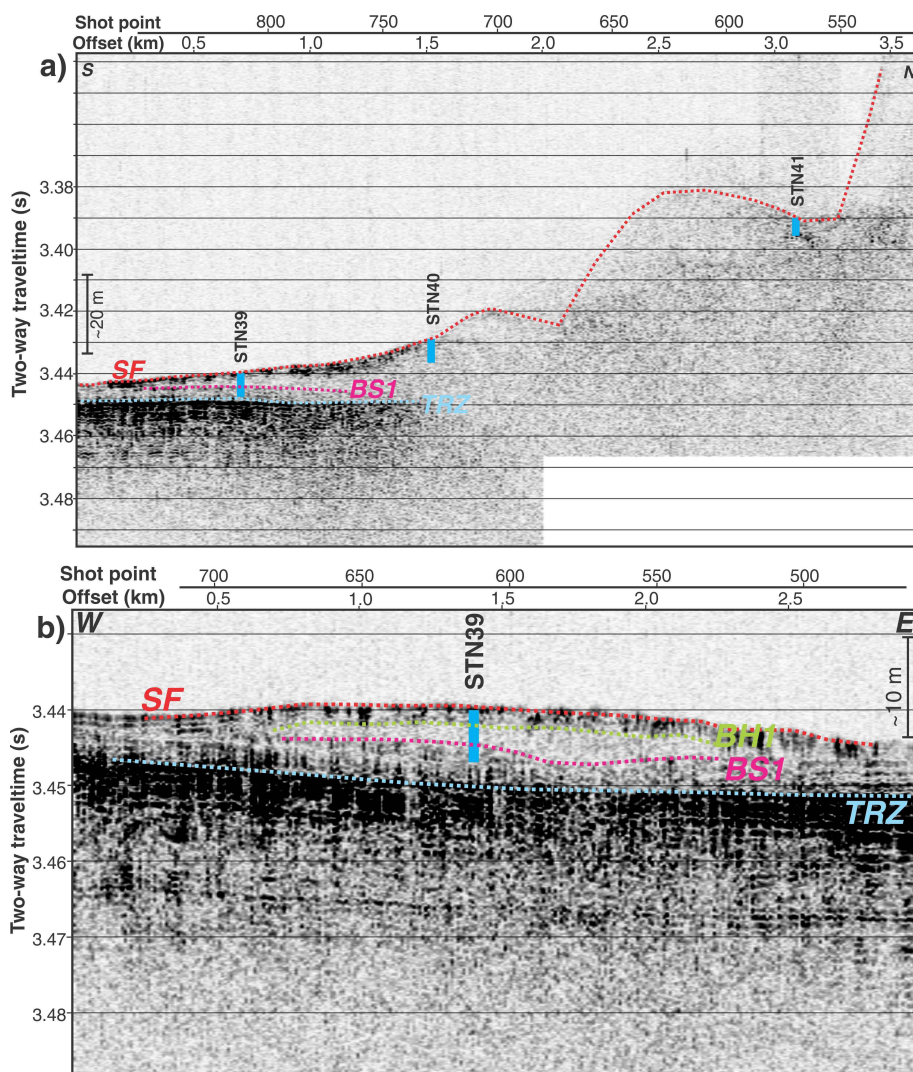
Figure 5. a) Subbottom profiler data acquired upslope of the slide mass through the coring transect of area 2 on the Juan de Fuca Plate with coring positions superimposed. **b)** Subbottom profiler data acquired through coring station station 39 of area 2 on the Juan de Fuca Plate with coring position superimposed. SF = seafloor (red), BH1 = base of Holocene sediments (green), BS1 = base of slump-mass 1(magenta), TRZ = top of reflective zone (light blue), STN = station

been deforming in response to subduction of the Juan de Fuca Plate beneath North America. The sediments incorporated into the slides are of glacial age, whereas the slides themselves date from seismic events that occurred much later. The lowermost debris flow at Otter slide was emplaced after 10 586 ± 87 BP and before 8077 ± 64 BP. Station 41 has only a short Holocene section and has no mixed Holocene and glacial sediments in the failed unit.

Stations 36, 37, and 38 all show apparent mixing of more recent olive sediments with the glacial slide material indicated by the textures and colours apparent in core images (Fig. 6, 7). In the case of the Otter slide, Holocene sediments are also incorporated into the slide mass in stations 39 and 40. The remolded nature of the slide material indicates that liquefaction did not occur, but the slides behaved as competent blocks that were mixed with sediments from overlying units. Slides show a variation regarding incorporation of overlying Holocene sediment.

Sediments appear to be more completely bioturbated in the upper unit at the Explorer Plate site (Fig. 7) compared to the Juan de Fuca Plate site (Fig. 6). This is possibly a

function of the more even sedimentation rate of 0.3–0.5 mm/a compared to a slower, but apparently more event-driven sedimentation rate at the Otter slide site where the hemipelagic sedimentation rate is about 0.2–0.3 mm/a.

Station 39 has six clearly defined turbidite sequences. Ages have been obtained on the uppermost four of these. The turbidite sequencess are numbered for ease of identification in Figure 7. The topmost turbidite was deposited after 1308 BP and before 1085 BP. The next turbidite downcore was deposited after 3846 BP. The third and fourth turbidite sequences are separated by a date of 8077 BP. The two basal turbidite sequences were deposited after 10 560 BP. The debris-flow unit dates from between 10 560 BP and 8077 BP. The debris flow in core stations 36 and 37 dates from after 8915 BP (station 36) and 9714 BP (station 37) and before 4988 BP (station 36).

Periodicity reported from Slipstream slide farther south indicates intervals between megathrust earthquakes of 394 ± 126 BP (Hamilton et al., 2015 and references therein). The present authors do not see each event recorded in the turbidite record on the Juan de Fuca site (Otter slide), so
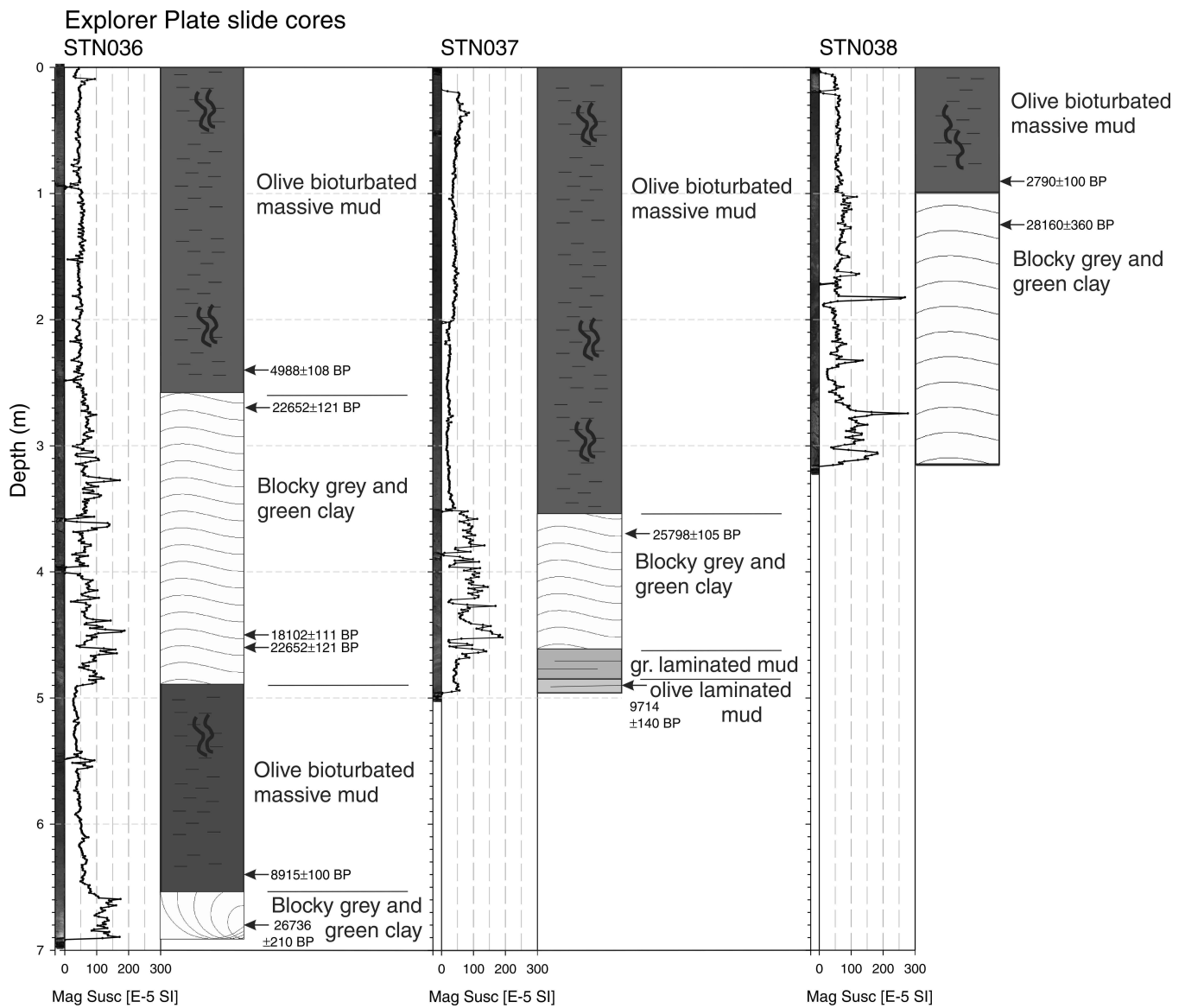
Figure 6. Cores 2013007PGC station 036, station 037, and station 038 collected at the Explorer Plate showing magnetic susceptibility, core image, core lithology, and radiocarbon ages of foraminifera in subsamples taken from the core (*see* Table 3 for details). No turbidite sequences were identified in cores from this slide area. Mag Susc = magnetic susceptibility, gr = grey, STN = station
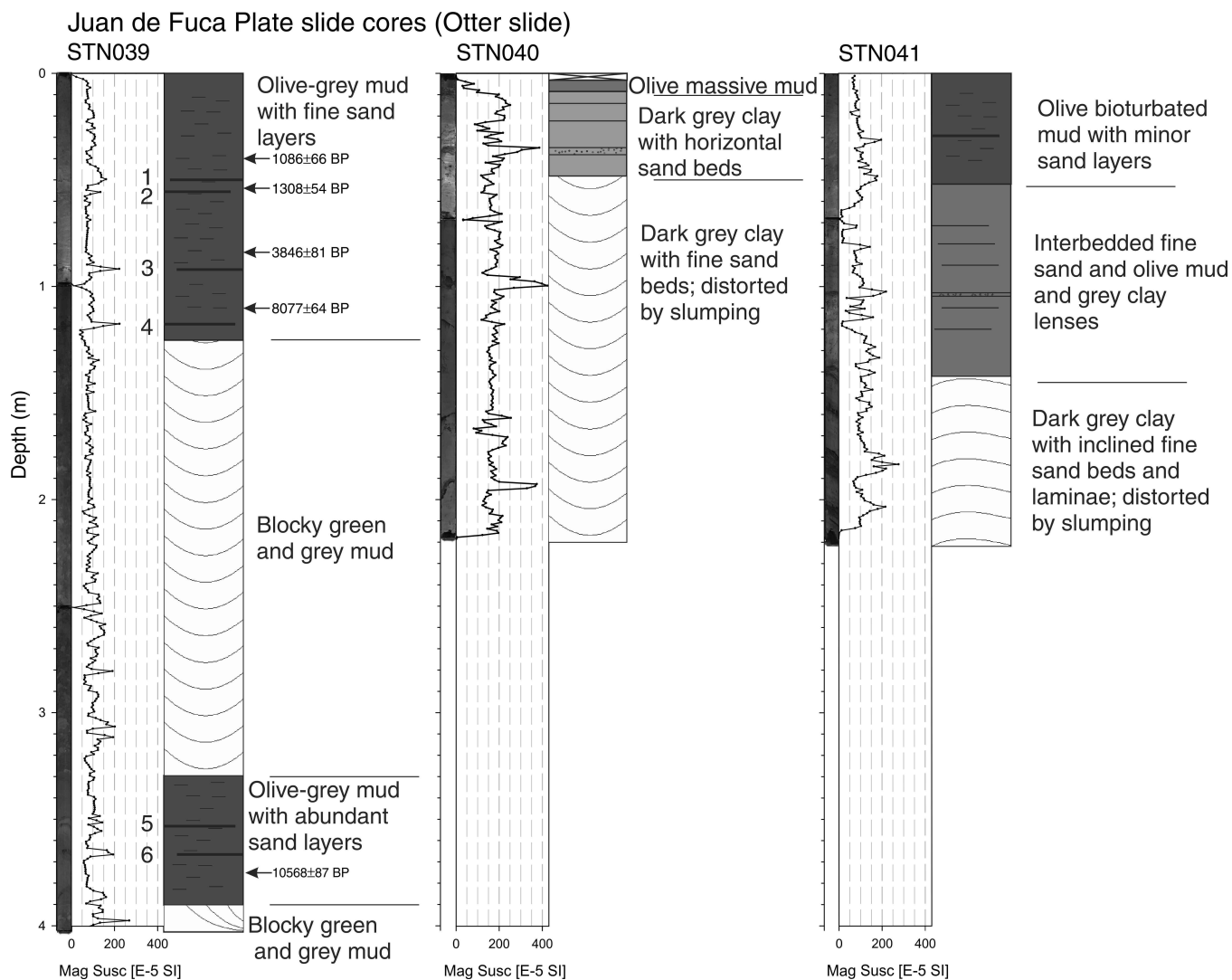
Figure 7. Cores 2013007PGC station 039, station 040, and station 041 collected at Otter slide on the Juan de Fuca Plate showing magnetic susceptibility, core image, core lithology, and radiocarbon ages of foaminifera in subsamples taken from the core (*see* Table 3 for details). Six turbidite sequences (numbered) were identified in station 039 from the distal slide area. Mag Susc = magnetic susceptibility, STN = station

it is obvious that many megathrust earthquakes were not recorded at this site. The age range of the turbidite sequences is interesting because only three events have been recorded after 8077 BP. It is possible that only the largest quakes have been recorded at the Otter slide site. The present authors would anticipate that as many as 10 turbidite sequences would be deposited after the 3846 BP date at 85 cm depth in core 39. Only three turbidite sequences are seen after this time. Qualitatively, the method can be used to gather data regarding large megathrust events. No turbidite sequences were seen in the Explorer Plate cores, which suggests that shaking does not occur related to large subduction zone rupture events. These results suggest that careful selection of coring sites and careful coring could construct a chronology of subduction events for northern Juan de Fuca Plate.

The underlying slide unit in the Explorer Plate cores was deposited after 8915 ± 100 BP and slightly before 4988 ± 108 BP. The older date is 1.5 m below the slide unit so the age of the slide can be constrained by applying the calculated sedimentation rate to both dates to give an age between about 5900 BP and 5400 BP.

CONCLUSIONS AND FUTURE WORK

Coring in carefully selected locations can sample deposits related to seismicity on the northern Juan de Fuca Plate. These preliminary results indicate that the Explorer Plate may not be subject to strong shaking related to megathrust earthquakes. The effort to establish a complete understanding of megathrust event effects on the Explore Plate will require further coring to examine sequences dating from time intervals known to host turbidite sequences from southern and central Cascadia studies. The record of recurring large Cascadia events is incomplete for Otter slide compared to sites from the central and southern margin. Other deformation front slides on the Juan de Fuca Plate might contain a more complete record of events, or several sites might serve as a composite paleoseismic record repository that could be examined in the future.

ACKNOWLEDGMENTS

REFERENCES

Adams, J., 1990. Paleoseismicity of the Cascadia Subduction Zone – Evidence from Turbidites off the Oregon-Washington Margin; Tectonics, v. 9, p. 569–583. doi:10.1029/TC009i004p00569

Bronk Ramsey, C., 2009. Bayesian analysis of radiocarbon dates; Radiocarbon, v. 51, no. 1, p. 337–360.

Davis, E., Currie, R., and Sawyer, B., 1987a. Acoustic imagery, northernVancouver Island margin; Geological Survey of Canada, Preliminary Map 13-1987, 1 sheet. doi:10.4095/133939

Davis, E., Currie, R., and Sawyer, B., 1987b. Acoustic imagery, southern Vancouver Island margin, Geological Survey of Canada, Preliminary Map 15-1987, 1 sheet. doi:10.4095/133941

Goldfinger, C., Nelson, C.H., and Johnson, J.E., 2003. Holocene earthquake records from the Cascadia subduction zone and northern San Andreas fault based on precise dating of offshore turbidites; Annual Review of Earth and Planetary Sciences, v. 31, p. 555–577. doi:10.1146/annurev.earth.31.100901.141246

Goldfinger, C., Nelson, C.H., Morey, A.E., Johnson, J.R., Patton, J., Karabanov, E., Gutierrez-Pastor, J., Eriksson, A.T., Gracia, E., Dunhill, G., Enkin, R.J., Dallimore, A., and Vallier, T., 2012. Turbidite event history — methods and implications for Holocene paleoseismicity of the Cascadia Subduction Zone; U.S. Geological Survey Professional Paper 1661-F, 170 p.

Hamilton, T.S., Enkin, R.J., Riedel, M., Rogers, G.C., Pohlman, J.W., and Benway, H.M., 2015. Slipstream: an Early Holocene slump and turbidite record from the frontal ridge of the Cascadia accretionary wedge off western Canada and paleoseismic implications; Canadian Journal of Earth Sciences, v. 52, no. 6, p. 405–430. doi:10.1139/cjes-2014-0131

Riedel, M., Novosel, I., Spence, G.D., Hyndman, R.D., Chapman, R.N., Solem, R.C., Lewis, T., and Zuelsdorff, L., 2006. Geophysical and geochemical signatures associated with gas hydrate related venting at the northern Cascadia margin; Geological Society of America Bulletin, v. 118, p. 23–38. doi:10.1130/B25720.1

Riedel, M., Côté, M.M., Manning, D., Middleton, G., Murphy, R., Neelands, P.J., Kodaira, S., Terada, T., Yamamoto, Y., and Saijo, T., 2014. Report of Cruise 2013008PGC, SeaJade-II Seafloor Earthquake Array Japan-Canada Cascadia Experiment, OBS deployment and piston coring of slope failures; Geological Survey of Canada, Open File 7716, 64 p. doi:10.4095/295552